

# Using data and model to infer climate and environmental changes during the Little Ice Age in tropical West Africa

Anne-Marie Lézine<sup>1</sup>, Maé Catrain<sup>1</sup>, Julián Villamayor<sup>1,2</sup> and Myriam Khodri<sup>1</sup>.

1. Laboratoire d'Océanographie et du Climat. Expérimentation et Approche numérique/IPSL. Sorbonne Université-CNRS-IRD-MNHN. 4 Place Jussieu. 75005. Paris. France

2. Department of Atmospheric Chemistry and Climate, Institute of Physical Chemistry Rocasolano, CSIC, Madrid, Spain.

## Abstract

Here we present hydrological and vegetation paleo-data extracted from 28 sites in West Africa from 5° S to 19° N and the past1000/PMIP4 IPSL-CM6A-LR climate model simulations covering the 850-1850 CE period to document the environmental and climatic changes that occurred during the Little Ice Age (LIA). The comparison between paleo-data and model simulations shows a clear contrast between the area spanning the Sahel and the Savannah in the North, characterized by widespread drought, and the equatorial sites in the South, where humid conditions prevailed. Particular attention was paid to the Sahel, whose climatic evolution was characterized by a progressive drying trend between 1250 and 1850CE. Three major features are highlighted: (1) the detection of two early warning signals around 1170 and 1240CE preceding the onset of the LIA drying trend; (2) an irreversible tipping point at 1800-1850CE characterized by a dramatic rainfall drop and a widespread environmental degradation in the Sahel; and (3) a succession of drying events punctuating the LIA, the major of which was dated around 1600CE. The climatic long-term evolution of the Sahel is associated with a gradual southward displacement of the Inter-Tropical Convergence Zone induced by the radiative cooling impacts of major volcanic eruptions that have punctuated the last millennium.

## 1. Introduction

Precipitation in tropical West Africa is closely related to the West African Monsoon (WAM) system, created by the temperature land-sea contrast between the tropical Atlantic and the west of the African continent (Nicholson 2013) and is also influenced by the migration of the Inter Tropical Convergence Zone (ITCZ, Gagdil 2018). The WAM long-term variability during the 20<sup>th</sup> century has focused much attention due to the severe consequences in the Sahel semi-arid region, which experienced a long period of drought in the 1970-80s (Folland et al. 1986; Giannini et al. 2003). It is broadly accepted that these changes were mainly driven by the sea surface temperature (SST) variability (Folland et al. 1986; Mohino et al. 2011; Rodríguez-Fonseca et al. 2015), amplified by land surface processes (Giannini et al. 2003; Kucharski et al. 2013). However, only a few works document the WAM variability prior to the 20<sup>th</sup> century (Nicholson et al. 2012; Gallego et al. 2015; Villamayor et al. 2018) due to the little information covering the 19<sup>th</sup> century and beyond. The paleo-archives are rare, often incomplete, and suffer from often poorly constrained chronologies. Moreover, these archives are rarely direct records of climate parameters, but indirect ones, namely historical, biological, or sedimentological. They integrate not only changes in environmental parameters but also

<sup>1</sup> Corresponding author : anne-marie.lezine@locean.ipsl.fr

45 the vital effect of species, the vulnerability or the resilience of ecosystems and the cultural  
 46 adaptations of populations. Here we use pollen and other environmental proxies as well as  
 47 historical chronicles to document the last millennium with a special focus on the period from  
 48 1250 to 1850 CE including the transition between the Medieval Climate Anomaly (MCA; 950-  
 49 1250CE) and the Little Ice Age (LIA; 1450-1850CE) periods characterised by global  
 50 temperatures respectively above and below average (Nash et al. 2016). The aim of this  
 51 research is not to record the climate variability at interannual scale but to discuss the timing,  
 52 distribution and magnitude of the major secular environmental changes which punctuated  
 53 the LIA in northern tropical Africa with a focus on the regional biomes and hydrological  
 54 systems responses times to rainfall anomalies.

## 55 2. Material and method

### 56 2.1 Paleo-data

57

58 This paper uses compilations of paleo-records from different sources with the highest  
 59 available resolution (Table 1; Fig. 1). These data have the advantage of providing continuous  
 60 records over the last millennium, but their temporal resolution is generally mostly  
 61 (multi)decadal to centennial: pollen data are used for vegetation reconstructions (Elenga  
 62 1992 ; Reynaud-Farrera et al. 1996; Ballouche 1998; Vincens et al. 1998; Salzmann et al. 2005;  
 63 Ngomanda et al. 2007; Waller et al. 2007; Brncic et al. 2009; 2017; Lézine et al. 2011; 2013;  
 64 2019; Lebamba et al. 2016; Tovar et al. 2019; Fofana et al. 2020; Catrain 2021), and  
 65 micropaleontological, sedimentological and geochemical data to capture hydrological and  
 66 climatic changes (Bertaux et al. 1998 ; Holmes et al. 1999 ; Street-Perrott et al. 2000 ; Schefuss  
 67 et al. 2005 ; Wang et al., 2008 ; Shanahan et al. 2009 ; Mulitza et al. 2010 ; Nguetsop et al.  
 68 2010 ; 2011 ; 2013 ; Carré et al. 2019 ; Lézine et al. 2019 ; Fofana et al. 2020 ; Catrain 2021).  
 69 Compilations of historical chronicles (Nicholson 1978; 1980; 2013; Nicholson et al. 2012;  
 70 Coquery-Vidrovitch 1997; Maley and Vernet 2013) and instrumental records (Gallego et al.  
 71 2015) have also been examined, although the first are based on records of extreme events  
 72 only (droughts, floods) and the second are limited in their temporal coverage. All these data  
 73 are also scattered in a few limited areas of the Sahel (Senegal, Southern Mauritania, Niger  
 74 River inner loop, Lake Chad basin) with possible redundancies.

75 The resulting data set is highly heterogeneous. Therefore, the data have been homogenized  
 76 as follows: (1) only records covering the interval between 900 CE and present day with at least  
 77 a 100-year temporal resolution have been taken into account, (2) in order to evaluate the  
 78 relative amplitude of the environmental/climate change, we build a 6-point scale ranging from  
 79 0, corresponding to the most arid environment (e.g., drying of lakes, salinization of water,  
 80 increase of dust transport, opening of the vegetation cover) or the driest climate, up to 6,  
 81 which refers to the most humid environment (e.g., high lake level, fresh water, dense  
 82 vegetation cover) or the wettest climate. Decimal values were punctually added to identify  
 83 minor changes in the paleoenvironment. This approach, based on our own expertise, provides  
 84 a *qualitative* description of regional environmental and climatic conditions. It emphasises the  
 85 major stages of environmental change while eliminating minor noisy variations (see  
 86 supplementary Figure).

87

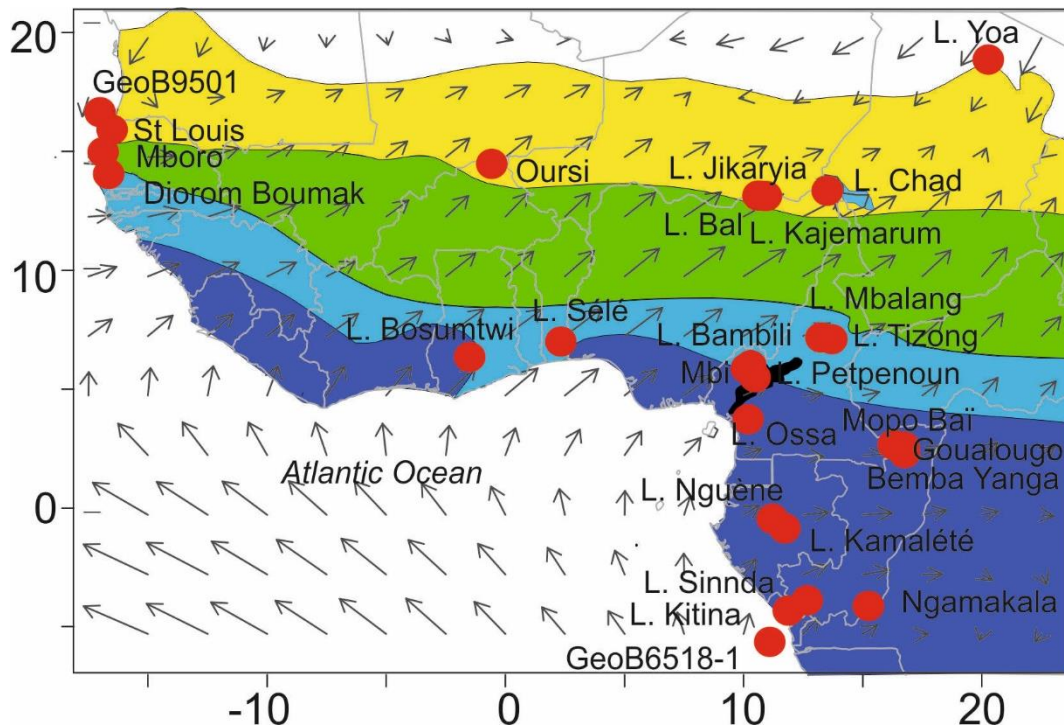
Site name	proxy	latitude	longitude	reference	Sector/vegetation zones
-----------	-------	----------	-----------	-----------	-------------------------

Lake Yoa	Pollen/sediment	19.057621	20.500690	Lézine et al. 2011	Sahara (Desert)
GeoB9501	Dust fraction	16.83333	-16.73333	Mulitza et al. 2010	Sahel
St Louis	Pollen/Diatom	16.03508	-16.48382	Fofana et al. 2020	Sahel (grasslands and wooded grasslands)
Mboro (Baobab)	Pollen/Diatom	15.149132	-16.909275	Lézine et al. 2019	Sahel (grasslands and wooded grasslands)
Oursi	Pollen	14.65283	-0.486	Ballouche 1998	Sahel (grasslands and wooded grasslands)
Dioron Boumak	Geochemistry	13.835809	-16.498372	Carré et al, 2019	Sahel/Savannah boundary
Lake Jikaryia	Sediment/Mineral-magnetic	13.3136667	11.077	Waller et al. 2007; Wang et al. 2008	Sahel (grasslands and wooded grasslands)
Lake Bal	Ostracods/Chemistry	13.304	10.943	Holmes et al. 1999	Sahel (grasslands and wooded grasslands)
Lake Kajemaru m	Dust fraction/Geochemistry	13.303	11.024	Street-Perrott et al. 2000	Sahel (grasslands and wooded grasslands)
Lake Chad	Historical	13.053472	14.463469	Maley and Vernet 2013	Sahel (grasslands and wooded grasslands)
Lake Mbalang	Pollen/Diatoms	7.316	13.733	Vincens et al. 2000; Nguetsop et al. 2011	Savannah
Lake Tizong	Pollen/Diatoms	7.25	13.583	Nguetsop et al. 2013; Lebamba et al. 2016	Savannah
Lake Sélé	Pollen	7.15	2.433	Salzmann et al. 2005	Savannah
Lake Bosumtwi	Geochemistry	6.5	-1.416	Shanahan et al. 2009	Central Africa (lowlands) (Equatorial forests)
Mbi	Pollen	6.089273	10.348549	Lézine et al., in press	Central Africa (highlands)

					(Afromontane forests)
Lake Bambili	Pollen/ Geochemistry	5.936	10.242	Lézine et al. 2013	Central Africa (highlands) (Afromontane forests)
Lake Petpenoun	Pollen	5.64147	10.64531	Catrain 2021	Savannah
Lake Ossa	Pollen/Diatoms	3.800	10.75	Reynaud Farrera et al. 1996; Nguetsop et al. 2010	Central Africa (lowlands) (Equatorial forests)
Mopo Bai	Pollen/Geochemistry	2.240	16.261388	Brncic et al. 2009	Central Africa (lowlands) (Equatorial forests)
Bemba Yanga	Pollen	2.18726	16.52513	Tovar et al. 2019	Central Africa (lowlands) (Equatorial forests)
Goualougo	Pollen	2.0875	16.54722	Brncic et al. 2017	Central Africa (lowlands) (Equatorial forests)
Lake Nguène	Pollen	-0.2	10.466	Ngomanda et al. 2007	Central Africa (lowlands) (Equatorial forests)
Lake Kamalété	Pollen	-0.7166	11.7666	Ngomanda et al. 2007	Central Africa (lowlands) (Equatorial forests)
Lake Sinnda	Pollen/Sediment	-3.836111	12.8	Bertaux et al. 1996 ; Vincens et al. 1998	Central Africa (lowlands) (Equatorial forests)
Ngamakala	Pollen	-4.075	15.38333	Elenga 1992	Central Africa (lowlands) (Equatorial forests)
Lake Kitina	Pollen/Sediment	-4.27	12	Bertaux et al. 1996 ; Elenga et al. 1996	Central Africa (lowlands) (Equatorial forests)
GeoB6518-1	Alkenone / Geochemistry	-5.588333	11.221667	Schefuss et al. 2005	Central Africa

88  
89  
90  
91

Table 1: Geographical positions, type and references of paleo-records used in this study (see Fig. 1).



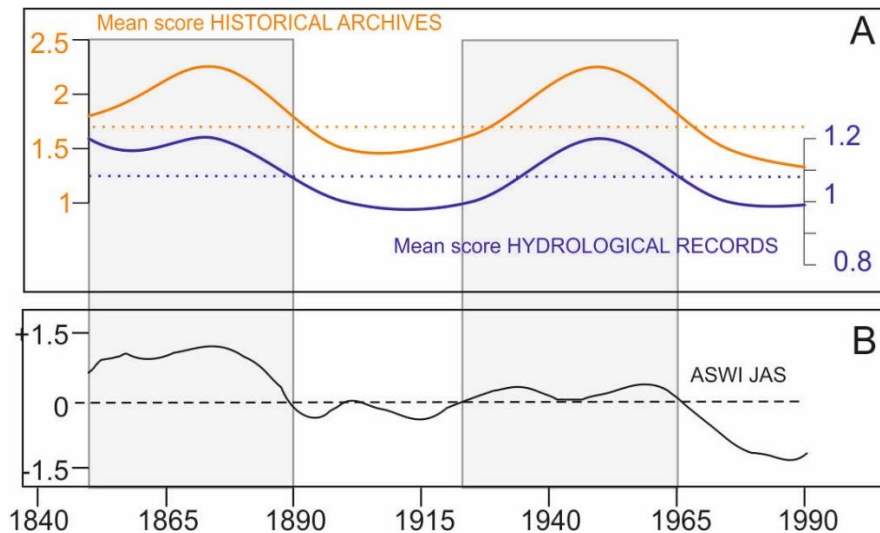
92  
93  
94  
95  
96  
97  
98  
99  
100  
101

**Figure 1:** Map showing the location of paleorecords available in tropical West Africa documenting the last millennium (Table 1). Grey arrows indicate the strength and direction of the main 925 hPa monsoonal winds during boreal summer, i.e., the WAM rainy season (NCEP-DOE AMIP-II Reanalysis (Kanamitsu et al., 2002)). In color, vegetation units from White (1983): dark blue: Guineo-Congolian rainforest; light blue: Sudano-Guinean woodland and wooded grassland (here referred to as Savannah (vegetation) zone); green: Sudanian woodland and wooded grassland; yellow: Sahelian grassland and wooded grassland. black: Afromontane forest.

102  
103  
104  
105  
106  
107  
108  
109  
110  
111  
112  
113  
114  
115  
116  
117

In order to verify whether the methodology employed provides reliable indications of environmental change for the period prior to the instrumental records scores of the WAM rainy season (July to September), multidecadal hydrological changes from natural archives and historical data (Table 1) in the Sahel are compared to the African Southwesterly Index (ASWI) developed by Gallego et al. (2015) over 1840-1990 CE. The ASWI is based on JAS wind direction data (i.e the persistence of the low-level southwesterly winds) from historical measurements available since 1839 in a region over the Atlantic, close to West Africa (29°W–17°W, 7°N–13°N). The ASWI is strongly correlated with the observed Sahel precipitation since 1900 and is, therefore, presented as a good indicator of its variability. It was validated against instrumental observations as a good measure of WAM intensity during the rainy season over the instrumental period (Gallego et al. 2015). Positive values of the ASWI indicate periods when the monsoon is well established over the Sahel, and thus define periods of heavy rainfall in the region, which is consistent with observational data (Descroix et al., 2015). Figure 2 shows strong similarities between our historical records and the ASWI. However, historical records give a slightly different magnitude of dry and wet anomalies that reflects the sensitivity of populations to periods of drought or flooding. Our assessment of hydrological

118 conditions based on natural archives reflects historical records variations but with a somewhat  
 119 weaker magnitude. This is probably due to the much lower temporal resolution of the  
 120 available data (25-50 yrs on average). It is also worth noting that the lake data corresponds  
 121 to a precipitation/evaporation balance and not the precipitation amounts at a given site.  
 122 Nevertheless, the curves are remarkably similar and point to wet periods centred ca 1875 and  
 123 1950 CE.  
 124



125  
 126

127 **Figure 2:** Observed and reconstructed rainfall anomalies over the Sahel during the 1840-1990  
 128 CE period. (A) the mean scores from historical (yellow curve) and natural archives (blue curve)  
 129 for the Sahel (Nicholson, 1978; 1980; Nicholson et al. 2012; 2013; Coquery-Vidrovitch, 1997;  
 130 Holmes et al., 1999; Street-Perrott et al. 2000; Waller et al. 2007; Wang et al. 2008; Mulitza et  
 131 al. 2010; Maley and Vernet, 2013; Lézine et al. 2019). The dotted yellow and blue lines  
 132 correspond respectively to the historical and paleohydrological archives mean scores during  
 133 the period 1850-1990CE. They allow identifying anomalously wet and dry periods. (B) The  
 134 African Southwesterly Index (ASWI) developed by Gallego et al. (2015) as a measure of rainfall  
 135 anomalies in Sahel during the WAM rainy season (July to September).  
 136

137

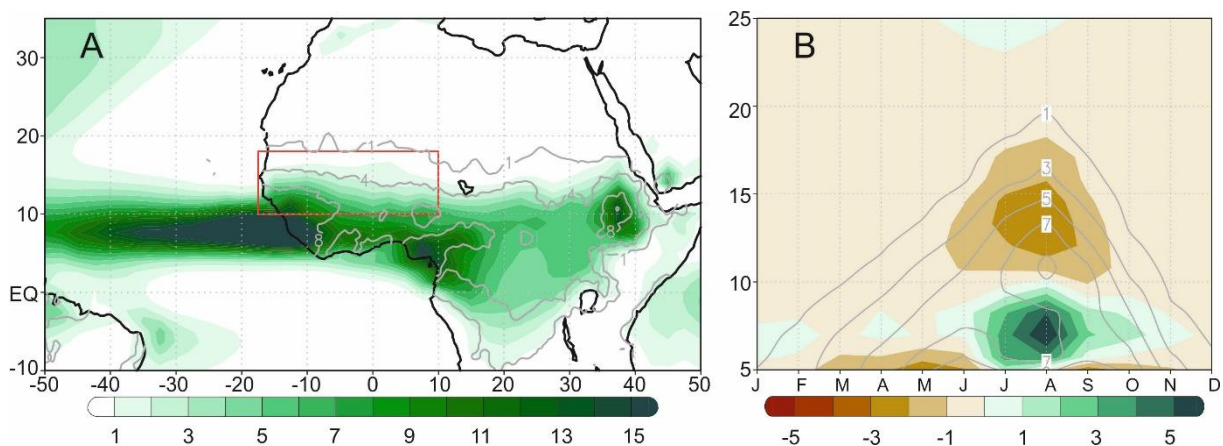
## 137 2.2 Model experiments

138 In this study we compare reconstructed environmental changes in Western Africa to those  
 139 simulated in the past1000 model experiment covering the 850-1850 CE climate performed as  
 140 part of 4<sup>th</sup> phase of the Paleoclimate Modelling Intercomparison Project (PMIP4; Jungclaus et  
 141 al. 2017; Kageyama et al. 2017) by the IPSL-CM6A-LR model version developed for the Coupled  
 142 Model Intercomparison Project phase 6 (CMIP6) at Institut Pierre-Simon Laplace (Boucher et  
 143 al. 2020; Lurton et al. 2020). The IPSL-CM6A-LR model couples the atmospheric component  
 144 LMDZ (Hourdin et al. 2020) to the land surface model ORCHIDEE (d'Orgeval et al., 2008) and  
 145 to the ocean model NEMO, which includes other models to represent sea-ice interactions  
 146 (Rousset et al., 2015) and biogeochemistry processes (Aumont et al. 2015). The atmospheric  
 147 and land-surface grid have a resolution of 2.5° in longitude and 1.3° in latitude with 79 vertical  
 148 layers. The oceanic component has 75 vertical levels with a mean spatial horizontal resolution  
 149 of about 1° and a refinement of 1/3° near the equator. This model reproduces fairly well the  
 150 ENSO (McPhaden et al. 2006) seasonality despite the sea surface temperature anomalies  
 151 extending too westward in the central Pacific during El Niño events. The spatial pattern of the

152 Atlantic Multidecadal Variability (AMV, Deser et al. 2010) teleconnection in the Pacific is  
 153 consistent with observations but the tropical Atlantic variability is relatively weaker. Unlike  
 154 most current state-of-the-art CMIP6 models, the IPSL-CM6A-LR model simulates a  
 155 predominant secular variability in the Atlantic with AMV peaks separated by about 200 years  
 156 (Boucher et al., 2020).

157 The past1000 IPSL-CM6A-LR model experiment is designed to simulate the climate response  
 158 to natural forcings recommended by PMIP4 (Jungclaus et al. 2017) and covering the pre-  
 159 industrial millennium (850-1849CE), namely the time varying astronomical parameters, the  
 160 trace gases (Meinshausen et al. 2017; Matthes et al. 2017), the eVolv2k volcanic forcing  
 161 (Toohey and Sigl 2017), the SATIRE-M 14C solar activity with an adaptation of the spectral  
 162 irradiance to the CMIP6 *historical* forcing and the land use forcing (Lawrence et al. 2016).  
 163 Three past1000 IPSL-CM6A-LR model simulations have been performed and branched off from  
 164 various initial conditions in a 600 years long spinup run with fixed external radiative forcing to  
 165 the year 850 CE. This spinup run, itself branched off from the IPSL-CM6A-LR pre-industrial  
 166 control (piControl) run with constant external radiative forcing, has been performed to avoid  
 167 any spurious drift in the past 1000 experiments that could be related to the adjustment of the  
 168 slow components of the climate system (such as the ocean), to the different radiative balance  
 169 at the beginning of the last millennium as compared to the pre-industrial levels.

170  
 171



172  
 173

174 **Figure 3:** Climatological bias of simulated monthly precipitation. A) JAS mean averaged across  
 175 (colors) the 2000-year piControl run and (contours) the 1891-2019 period in GPCPv2020  
 176 observational database. B) (colors) Meridional seasonal cycle of the 10° W – 10°E mean model  
 177 bias (simulation minus observations) compared to (contours) the GPCPv2020 climatology. All  
 178 units are mm/day. Red box in (A) indicates the Sahel region (17.5°W-10°E; 10°-18°N).

179

180 The IPSL-CM6A-LR model reproduces the observed climatological distribution of maximum  
 181 rainfall across West Africa during the WAM rainy season (Fig. 3A). The timing of the simulated  
 182 WAM seasonal cycle is also in good agreement with observations, with a well-defined onset  
 183 of the rainy season in July and then a demise after September (Fig. 3B). However, the  
 184 northward shift of maximum rainfall over the Sahel during the rainy season is underestimated  
 185 by the model by about 4° (the model's maximum in August is ~7°N and the observed one at  
 186 11°N). As a result the climatological rain belt over West Africa is slightly more constrained to  
 187 tropical regions compared to observations and dryer Sahel on average. However, the well-



188 characterized WAM seasonal timing suggests that there are no remarkable biases affecting  
189 the simulated precipitation variability.

190 Then, to characterize the simulated Sahel rainfall multidecadal variability over the past  
191 millennium and contrast to the reconstructed environmental series, an index is calculated as  
192 the 10-year low-pass-filtered Sahel precipitation anomalies in the rainy season from past1000  
193 simulations. Seasonal precipitation anomalies from July to September (JAS), relatives to the  
194 piControl climatology, are area-weighted and averaged across the Sahel region (red box in Fig.  
195 3A), then filtered with a 10-year centered moving mean with truncated endpoints (i.e., only  
196 averaging existing elements within the 10-year window). An ensemble-mean index is also  
197 performed to highlight the forced component of the Sahel multidecadal variability in response  
198 to natural forcings that are common to the three past1000 members, such as the effect of  
199 large volcanic eruptions, in contrast to the internal variability.

200

### 201 **3. Results**

#### 202 **3.1 The hydrological records**

203

204 The hydrological records provide a contrasting picture from one region to another: the Sahel,  
205 the Sudano-Guinean Savannah zone and the tropical forests. They also reveal some local  
206 exceptions. As already noted (e.g., Vincens et al. 1999), the local hydrogeological context may  
207 strongly affect the individual response of lakes and wetlands to rainfall variations and partly  
208 explains this apparent heterogeneity.

209 The main characteristics of the hydrological evolution in the Sahel, in the Savannah zone and  
210 in low- and high-altitude equatorial forests can be summarized as follows (Fig. 4):

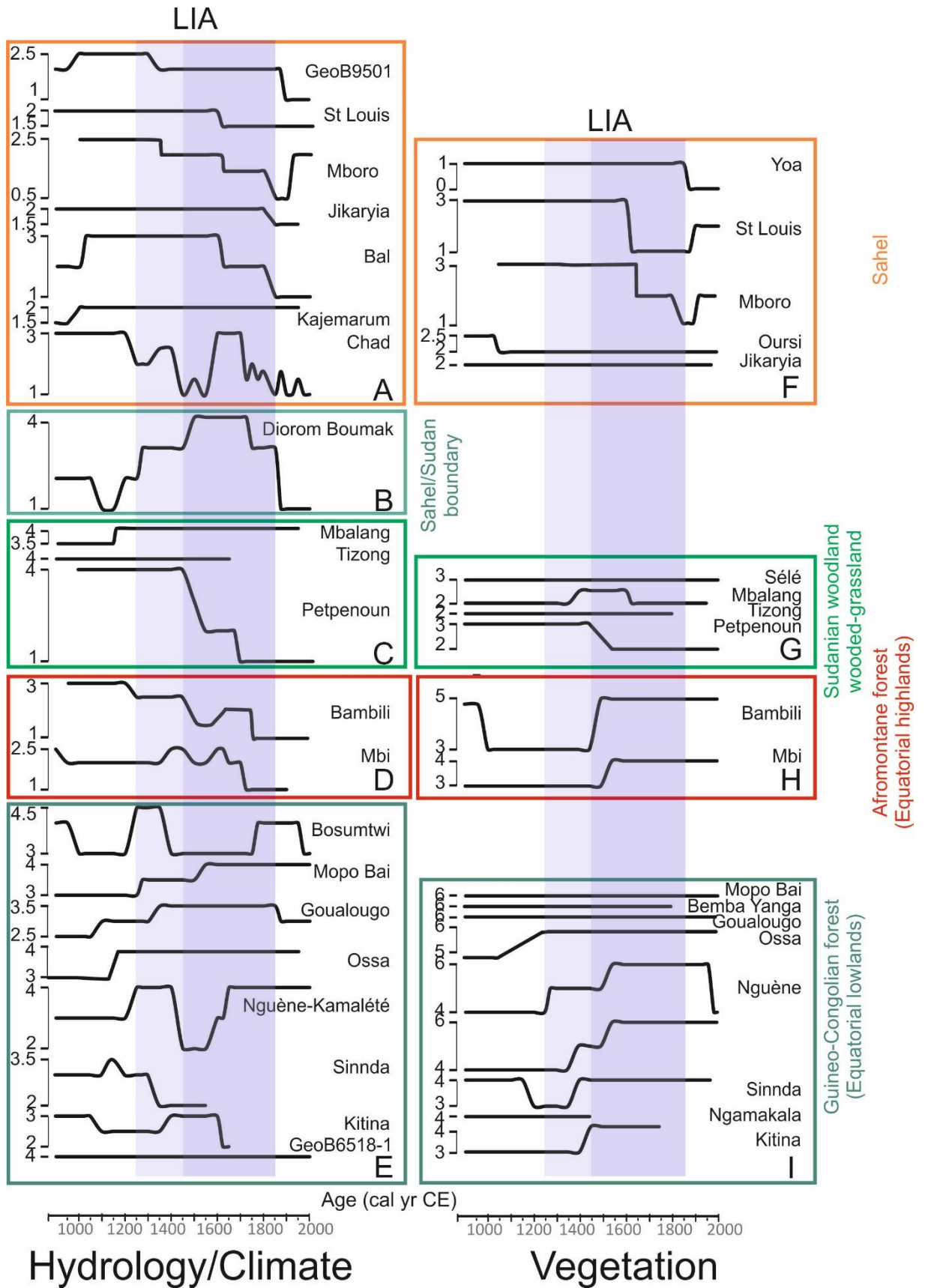
211 • Data from the central and western Sahel (Fig. 4A) point to a relatively dry period at the  
212 end of the first millennium (900CE) at Bal, Kajemarum and in the Senegal River  
213 watershed (GeoB9501). A wet period followed, already present at Mboro near the  
214 littoral, which lasted up to 1350CE. Except at Kajemarum and Jikarya, where  
215 hydrological conditions remained relatively stable, a gradual trend toward increased  
216 aridity is recorded in two steps dated ca. 1625CE and 1800CE, respectively. Then,  
217 during the last two centuries, only minor fluctuations occurred in a general context of  
218 widespread aridity.

219 In the lake Chad area, Maley and Vernet (2013) depict a rather different and complex  
220 history probably due to the variety of the archives they used (both historical and  
221 natural) and also to the complexity of the hydrology of this immense water body  
222 (Pham-Duc et al. 2020) fed by underground waters and by rivers of distant  
223 geographical origin. The authors identify two major periods of flooding in the lake  
224 Chad area: from the onset of the millennium to ca. 1200CE, then between 1600 and  
225 1700CE, with a series of dry periods in between then from 1700CE onwards.

226 • Only three sites document the hydrological evolution of the Savannah zone south of  
227 the Sahel (Fig. 4C). These sites are located in the centre of the savannah zone (White  
228 1985): two crater lakes on the Adamawa plateaus (Mbalang and Tizong) and the other  
229 at the mouth of the tributary of Lake Petpenoun in the Grassfields region of Cameroon.  
230 The Adamawa lakes do not show any significant hydrological changes throughout the  
231 last millennium. In contrast Petpenoun records a clear evolution towards aridity which  
232 started ca. 1425CE and culminated ca. 1650CE up to the present day.



- 233 • Diorom Boumak (Fig. 4B) is situated at the southern boundary of the Sahel, in the  
234 littoral mangrove of the Saloum estuary. In contrast to the other sites from the Sahel  
235 and savannah zone this site records a remarkable wet period between 1500CE and  
236 1800CE. As elsewhere however, aridification started ca. 1800CE.
- 237 • The equatorial lowlands is characterized by contrasting hydrological situations  
238 reflecting the diversity of local hydrogeological settings (Fig. 4E). Low lake levels are  
239 recorded at Bosumtwi, Mopo Bai, Goualougo, Nguène-Kamalété and Ossa during a  
240 period centred around 1100CE in contrast to Sinnda and Kitina where moist conditions  
241 occurred. Moisture increased as soon as 1350CE at Goualougo and continued up to  
242 1400CE at Mopo Bai and Kitina. Then, there is a clear opposition between Sinnda,  
243 Nguène-Kamalété and Bosumtwi where low lake levels occurred during a dry phase  
244 between ca 1350 and 1700CE and Mopo Bai, Goualougo, Ossa and Kitina, which are  
245 characterized by wetter conditions. In any case, the marine record at the mouth of the  
246 Congo River (GeoB6518-1) suggests that all these hydrological variations in the  
247 equatorial lowlands remained of relatively low amplitude.
- 248 • In the Cameroon highlands (Fig. 4D), hydrological conditions steadily declined as  
249 shown at lake Bambili, starting from ca. 1250 and culminating ca. 1675CE. This gradual  
250 trend is interrupted ca. 1500CE by a more pronounced phase of lake level lowering.  
251 The Mbi swamp displays a rather different pattern: here, the water level was relatively  
252 low throughout the whole last millennium except to two discrete wetter phases ca.  
253 1450 and 1650CE.  
254



255  
256  
257  
258  
259

**Figure 4:** Mean scores of hydrological and vegetation changes along a North-South transect from the northern limit of the Sahel (Yoa) to the Congo basin (GeoB6518-1). Data are grouped within the phytogeographical entities defined by White (1983) in tropical Africa: Sahelian

260 grassland and wooded grassland, Sudano-Guinean savannah, highland Afromontane forest,  
 261 lowland Guineo-Congolian forest. The shaded vertical bands indicate the transition period  
 262 between the medieval climate anomaly and the Little Ice Age (1250-1450CE light shading) and  
 263 the LIA (1450-1850CE dark shading).

264

### 265 **3.2 Pollen data**

266

- 267 • In the open landscapes of the Sahara, Sahel and Savannah zones, vegetation changes  
 268 were of minor amplitude except at sites where gallery forests were previously well  
 269 developed. It is in the westernmost part of the Sahel that the most profound changes  
 270 in vegetation cover are recorded : In the Niaye area (Mboro) and in the Senegal river  
 271 delta (St Louis), the degradation of the landscape originated ca. 1300CE and  
 272 accelerated ca. 1600CE to a maximum reached ca. 1850CE (Fig. 4F). A discrete  
 273 vegetation recovery is then recorded in the 19th century. In contrast, sites from the  
 274 central Sahel (Oursi and Jikarya) remained relatively stable throughout the last  
 275 millennium in spite of a slight degradation recorded at Oursi ca. 1050CE. North of the  
 276 Sahel (Yoa), the aridification of the desert landscape accelerated from the 19th century  
 277 onward. South of the Sahel, in the Savannah zone, lakes Tizong and Sélé do not record  
 278 any marked environmental change contrary to Petpenoun where a slight degradation  
 279 is recorded ca. 1425CE (Fig. 4G). At Mbalang, a discrete phase of vegetation recovery  
 280 occurred between ca 1400-1600CE.
- 281 • The forest cover remained roughly unchanged in the central forest massif (Mopo Bai,  
 282 Bamba Yanga, Goulalougo, Fig. 4I). In the western regions by contrast, (Ngamakala,  
 283 Kitina, Lac Ossa, Nguène and Kamalété the forest gradually developed since 1250-  
 284 1350CE in spite of the discrete hydrological fluctuations. In the Cameroon highlands  
 285 (Fig. 4H), the forest development occurred later, ca 1550-1500CE, after a phase of  
 286 forest clearance from 1000 to 1450CE.

287

### 288 **3.3 Model results**

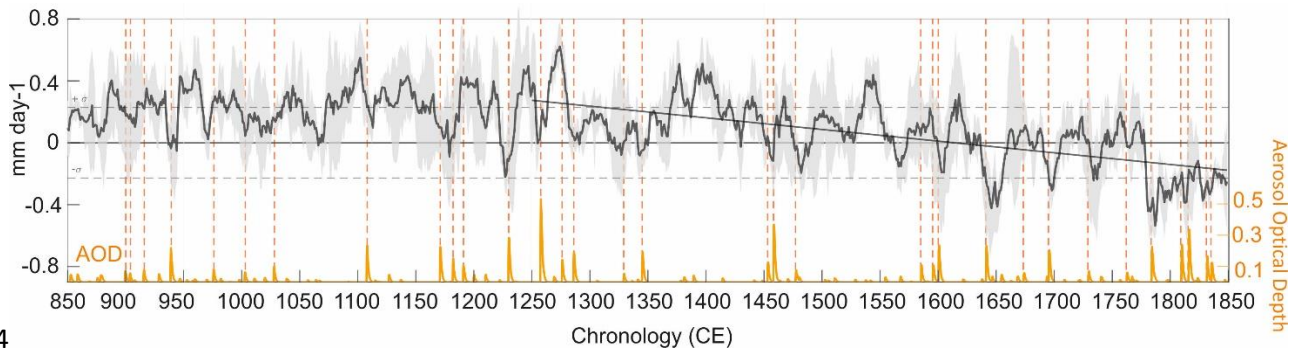
289

290 The index of the ensemble-mean Sahel JAS precipitation simulated over the past millennium  
 291 reveals a change from a relatively wet mean state in the MCA (950-1249 CE) to a drier one in  
 292 the LIA (1450-1849) (Fig. 5), suggesting a shift of the average WAM rainfall regime. Such  
 293 continuous decline presents a linear rate of the seasonal Sahel rainfall of -0.7 mm per decade  
 294 over 1250-1849CE, resulting in a 7% loss of the mean precipitation in the LIA relative to MCA  
 295 (Fig. 5). Regarding decadal variations, the ensemble-mean index of past1000 Sahel  
 296 precipitation almost doubles its variability in the LIA with respect to the MCA (the variance in  
 297 859-1249CE is 51% higher than in 1450-1849CE), which suggests a more unstable rainfall  
 298 regime, apart from drier on average, by the late past millennium in response to natural  
 299 external forcings. Such a simulated long-term drying trend and increased LIA Sahel  
 300 precipitation decadal variability is related to the volcanic forcing influence on SSTs, which  
 301 integrates the induced radiative cooling (Fang et al. 2021). The more frequent large volcanic  
 302 eruptions during the LIA, as compared to the MCA, is integrated by the ocean long memory,  
 303 leading to a gradual SST decrease that is more pronounced in the Northern Hemisphere than  
 304 the Southern Hemisphere. The relative North Atlantic SST cooling trend along 850-1849CE,  
 305 gradually promotes a southward shift of the Inter-Tropical Convergence Zone (ITCZ) and a  
 306 weakening of monsoon moisture inflow to Western Africa. The long term WAM weakening is

307 further amplified in the few years following any new large volcanic event, which occurrences  
 308 are indicated by the vertical dotted lines on Figure 5. As a consequence, more frequent  
 309 negative rainfall anomalies lasting at least 5 consecutive years are also evident during the LIA  
 310 as compared to the MCA, with significant drying that can persist up to 60 years around clusters  
 311 of eruptions such as those of the 19th century.

312

313



314

315

316 **Figure 5:** Multidecadal Sahel rainfall variability in IPSL-CM6A-LR past1000 simulations. Black  
 317 line: 10-years low pass filtered index of Sahel JAS precipitation anomalies averaged in boxed  
 318 area in Figure 3 (i.e.,  $10^{\circ}$ - $18^{\circ}$ N and  $17.5^{\circ}$ W- $10^{\circ}$ E). The black line corresponds to the ensemble  
 319 mean, the grey shading to the ensemble spread and diagonal line to the 1250-1849 CE linear  
 320 fit. Dashed horizontal lines show the +/- standard deviation of the equivalent piControl index.  
 321 The volcanic forcing used in the IPSL-CM6A-LR model experiments is shown by the orange  
 322 curve as the globally averaged Aerosol Optical Depth (AOD). Red vertical dotted lines indicate  
 323 the occurrence of strong volcanic eruptions about the size or larger that the Pinatubo eruption  
 324 (June 1991) defined when the tropical ( $20^{\circ}$ S- $20^{\circ}$ N) or northern extratropical ( $50^{\circ}$ N- $90^{\circ}$ N)  
 325 mean AOD is larger than 0.1.

326

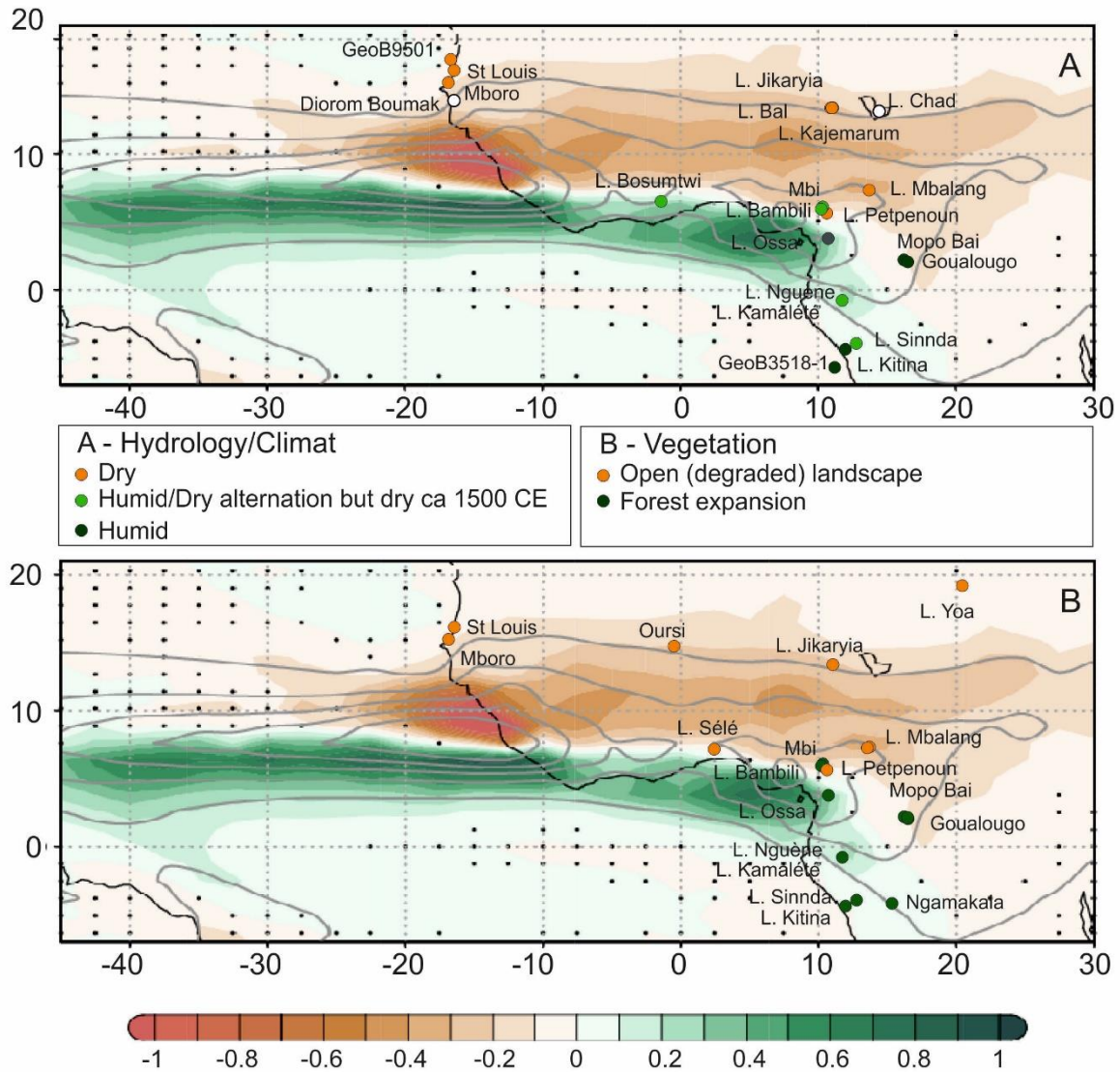
## 327 4. Discussion

328

### 329 4.1 Hydrology and Climate changes at secular timescale

330

331 Data and past1000 model simulations show a strong North-South contrast between the Sahel  
 332 and Savannah zones, both subjected to severe drying during the LIA, and the equatorial areas,  
 333 spanning the Gulf of Guinea coast, suggesting an overall change of the WAM.



334  
335

336 **Figure 6:** Distribution of JAS rainfall anomalies difference between the LIA (1450-1849 CE) and  
337 the MCA (950-1249 CE) as simulated by the IPSL-CM6A-LR model in the past1000 ensemble-  
338 mean (shading,  $\text{mm day}^{-1}$ ) compared to hydrological/dust (A) and vegetation (B) paleorecords  
339 during the LIA shown as dots following the same color scale as simulated anomalies. Grey  
340 contours indicate the piControl climatology from  $2 \text{ mm day}^{-1}$  in intervals of  $4 \text{ mm day}^{-1}$ .  
341 Stippling indicates disagreement across the three past1000 members on the sign of the  
342 represented difference.

343

344 The difference between the simulated past1000 JAS precipitation during the LIA and the MCA  
345 shows a characteristic distribution of a weakened WAM associated with a southward shift of  
346 the ITCZ, with less rainfall across the Sahel and more in the Gulf of Guinea coast (Fig. 6). These  
347 simulated anomalies are consistent with the overall distribution of hydrological and  
348 vegetation proxy reconstructions.

349

#### 350 4.1.1 Hydrology

351

352 Three major regions can be recognized from the paleohydrological records: The Sahel and  
353 Savannah zones, with drying trend; the center of the Congo Basin, which exhibit an opposite  
354 trend of increasing humidity; and the boundary between the dry and humid domains defined  
355 by the equatorial sectors closest to the coast or in mountain, where an alternation of wet and  
356 dry phases is recorded. Two paleo-records differ from this general picture: that of Lake Chad,  
357 where a period of flooding is recorded ca 1600CE, and that of the Diorom Boumak, where the  
358 LIA is entirely characterized by a wet period (Fig. 4). As evoked above, the multiple origins of  
359 the data and the complex hydrological system of Lake Chad may have introduced a bias into  
360 the hydrological record and may explain (at least partly) the difference with the other Sahelian  
361 archives. It is also likely that the rivers that feed the lake, which originate from southern  
362 regions (the Chari and Logone rivers and their tributaries), may have caused an influx of water  
363 during the short humid phase recorded on the Cameroon highlands (Bambili and Mbi) ca  
364 1600CE. The case of the Diorom Boumak site is more complex: the historical records  
365 mentioned by Maley and Vernet (2013) or Carré et al. (2019), among others, indicate that the  
366 Saloum sector was wetter than the rest of the Sahel during part of the 16th century, allowing  
367 for the establishment of two harvests per year. This may have been due, according to Maley  
368 and Vernet (2013), to the occurrence of two rainy seasons, one in the core of the WAM season  
369 in summer and another (usually of lesser importance) referred as “Heug rains” linked to polair  
370 air intrusions in winter (Le Borgne 1979).

371

#### 372 **4.1.2 Vegetation**

373

374 In the central Sahel, already degraded prior to the LIA (Lézine 2021), such as at Oursi, no  
375 significant change occurred in the vegetation landscape which remained open throughout the  
376 last millennium (Fig. 4B). The same pattern is observed in the wettest areas of the Congo Basin,  
377 where the forests remained unchanged in composition and physiognomy (Tovar et al. 2019).  
378 Elsewhere in the forest galleries of the Sahel and the Savannah zone (Mboro, St. Louis,  
379 Petpenoun) the evolution of vegetation mirrored that of hydrological conditions while  
380 recording a gradual degradation that culminated around 1800-1850 CE. In the westernmost  
381 sector of the Sahel (Mboro, St Louis), the data suggest however a slight recovery of the  
382 vegetation cover during the last few decades.

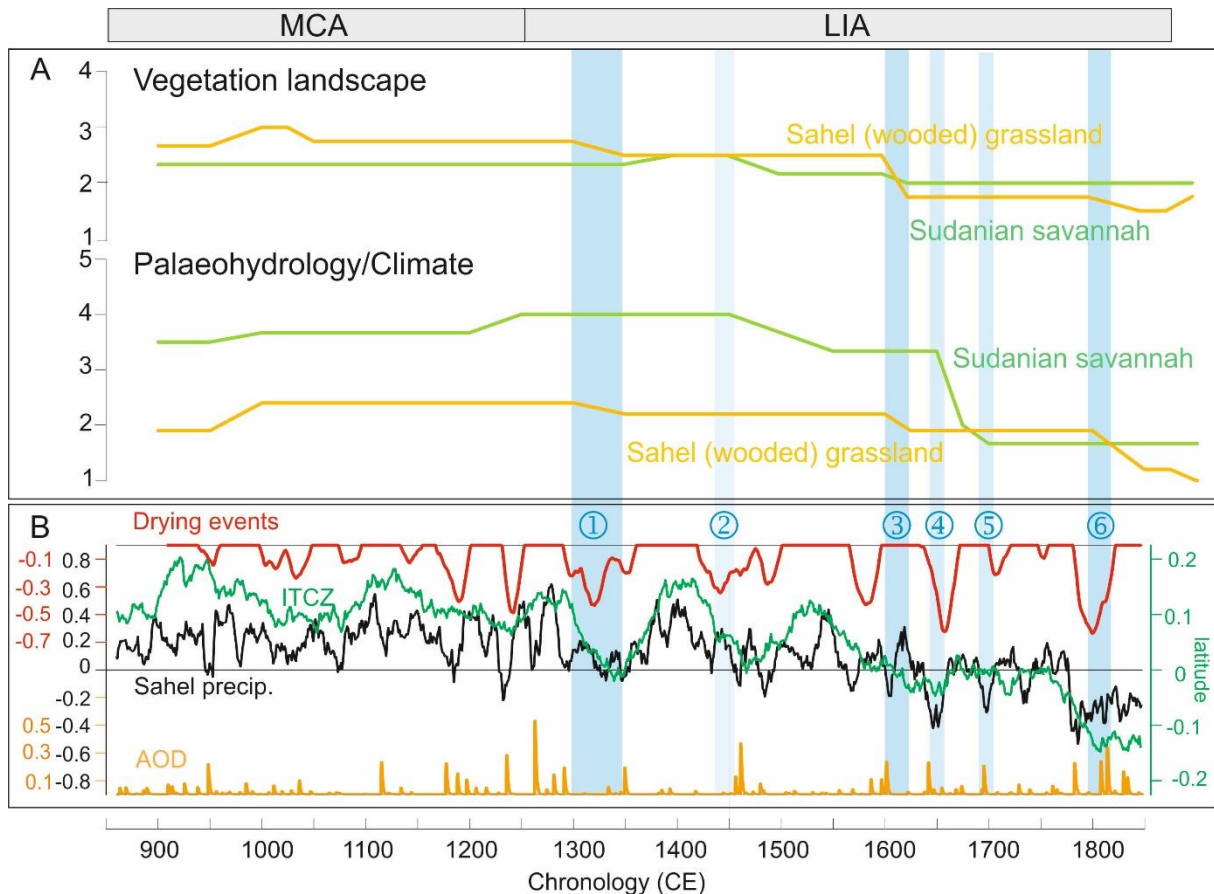
383 In contrast, both high and low elevation sites from the equatorial forest regions show an  
384 opposite trend with marked forest recovery that began in the early years of the LIA and  
385 accelerated around 1450CE. The forest expanded in the Equatorial lowlands despite increased  
386 human presence has already been noted by Vincens et al. (1999). That means that the local  
387 hydrological variations, and particularly the 1500 CE dry event, were of too small an amplitude  
388 to impact forest dynamics. At most, a plateau in forest recovery is observed at that time  
389 (Nguène, Kamalété). While the forest recovery was gradual at low altitudes, it seems to have  
390 occurred more abruptly in the highlands.

391

#### 392 **4.2 The chronology of events at multidecadal timescale: focus on the Sahel and Savannah** 393 **zone**

394





395  
 396 **Figure 7:** Multiproxy records of hydrology and vegetation during the last millennium in the  
 397 driest biomes (Sahel and Savannah zone) in western Africa (A) and long-term evolution of  
 398 rainfall over the Sahel as simulated by the IPSL-CM6A-LR past1000 model (B). Panel B: (Black  
 399 line) 10-year filtered ensemble-mean Sahel precipitation index ( $\text{mm day}^{-1}$ ). (Green line) 50-  
 400 year filtered anomalous latitudinal position of the JAS ITCZ (defined as the latitudinal  
 401 maximum zonal-mean rainfall in  $40^{\circ}\text{W}$ - $10^{\circ}\text{E}$ ) in the past1000 simulations respectively to the  
 402 piControl JAS mean position (in degrees of latitude). (Orange line) Global-mean AOD (volcanic  
 403 forcing). (Red line) Sahel Drying Persistence Index defined as the 50-year running negative  
 404 trend values over the Sahel ensemble-mean JAS precipitation index ( $\text{mm day}^{-1}$  per 50 years).  
 405 Blue bars and numbers highlight the main climate/environmental degradation thresholds  
 406 identified in the paleo-records.

407  
 408 Environmental changes in the Sahel and Savannah zones during the LIA occurred in the context  
 409 of widespread environmental degradation that followed the severe environmental crisis at  
 410 the end of the African Humid Period (AHP; deMenocal et al., 2000). Between 3300 and 2500  
 411 cal yr BP (Lézine, 2021), the forests and woodlands, that widely expanded across the plains  
 412 and mountains of West Africa, strongly declined. This is particularly striking along the Atlantic  
 413 coast of Senegal, between  $15^{\circ}$  and  $17^{\circ}$  N where specific environmental conditions related to  
 414 the proximity of the sea and the presence of a water table near the surface favored the  
 415 development of exceptionally dense forest galleries of humid tropical affinity during the AHP  
 416 (Lézine 1989). As a result of this major environmental crisis, the Sahel and Savannah zone took  
 417 on its modern aspect of semi-desert grassland and wooded grassland. In this context,  
 418 discernible environmental fluctuations, particularly in vegetation, are of limited magnitude,  
 419 with the exception of sectors where forest galleries were widely established during the AHP.  
 420



421 To discuss the chronology of events that punctuated the LIA, paleo-data were averaged in  
 422 each geographical area (Sahel, Savannah zone) in the two categories covered by our study:  
 423 hydrology/climate and vegetation (Fig. 7A). A Drying Persistence Index was constructed from  
 424 our model results in order to quantify the Sahel precipitation deficit over at least 50-year  
 425 periods (red curve in Fig. 7B). It is defined at each year as the negative linear trend of the Sahel  
 426 ensemble-mean JAS precipitation (black curve in Fig. 7B) across the 50 previous years. We use  
 427 50 years to be consistent with the multi-decadal to centennial temporal resolution of the  
 428 paleo-data.

429 The past1000 simulations represent several drying events of various amplitude and duration  
 430 during the MCA that do not correspond to any major change in the vegetation of the Sahel  
 431 and Savannah zone. Instead, the environment in these two areas appears to be characterized  
 432 by a relatively stable humid regime (Fig. 7A). This is coherent with the rainy mean state  
 433 represented by the past1000 simulations over the MCA, which is associated with an  
 434 anomalous northward ITCZ position (green curve in Fig. 7B) all over this period compared to  
 435 the LIA.

436 At the end of the MCA, two early warning signals (Lenton 2011) of Sahel drying events centred  
 437 at 1170 and 1240 CE are identified in our model experiments. The intensity and brevity of  
 438 these two events contrast with the minor dry phases identified prior to the LIA since the onset  
 439 of the last millennium. The Drying Persistence Index at these two events, which timing  
 440 coincides with the occurrence of large clusters of volcanic eruptions (orange curve Fig. 7B),  
 441 reaches over  $-0.3 \text{ mm day}^{-1}$  across 50 years. Both events preceded the onset of the LIA gradual  
 442 drying trend starting at 1250CE. This drying trend was sustained by the southward migration  
 443 of the ITCZ which shifts south of the piControl mean position at 1600 CE. It is consistent with  
 444 the continuous degradation of hydrological and vegetation conditions since 1250 CE in the  
 445 Sahel and Savannah zone identified in our multi-proxy records.

446 Several abrupt drying events larger than those identified during the MCA punctuated the LIA,  
 447 some of which reaching over  $-0.5 \text{ mm day}^{-1}$  across 50 years. Despite the difference in temporal  
 448 scale between the two approaches used here, there is a striking agreement between the major  
 449 simulated droughts and the environmental degradation steps in our paleorecords (blue bars  
 450 in Fig. 7). These degradation periods, in turn, span the largest eruptions from ca. 1250 to ca.  
 451 1850CE, which are associated with the multi-decadal variability of Sahel precipitation over the  
 452 past millennium in PMIP4 multi-model experiments.

#### 453 **4.2.1 Steps in the degradation of the climate and the environment in the Sahel**

454 Three major steps are identified:

- 455 - The first dramatic environmental degradation occurred between 1290 and 1350 CE  
 456 (event 1), i.e., ca. 50 years after the first warning signal and lasted about 60 years. Dust  
 457 fluxes to the ocean, which had stabilized during the medieval warm period, increased  
 458 (Mulitza et al. 2010) whereas lake levels dropped in the interdunal depressions in the  
 459 western Sahel leading to the salinization of the waters (Lézine et al. 2019).
- 460 - The second stage in the degradation of environmental conditions occurred ca 1600CE  
 461 (event 3). The environmental degradation was common to the entire Sahel (Bal,

462 Mboro, St Louis) while corresponding to a major collapse of the forest galleries at  
 463 Mboro. Here also, a time lag of ca. 50 years can be observed between the onset of a  
 464 drought phase and the response of the vegetation.

465 - The ultimate environmental threshold is recorded ca 1800CE (event 6). It resulted in  
 466 the widespread lowering of lake levels, the massive contribution of dust to the ocean,  
 467 and the irreversible destruction of forest galleries in the western Sahel in response to  
 468 an abrupt drop in rainfall ca 1800CE, already observed by Carré et al. (2019) in the  
 469 Saloum river delta. By accounting for a catastrophic decrease in precipitation of  $-0.6$   
 470  $\text{mm day}^{-1}$  over 50 years in our model experiments, this climatic tipping point related  
 471 to closely spaced large volcanic eruptions (starting with Laki eruption in 1783 CE  
 472 followed by the eruptions cluster over the 1809-1835 CE period including the 1815  
 473 Tambora event), at the origin of the modern environmental conditions in the Sahel,  
 474 was twice as large as the early warning signals identified at the end of the MCA.

475 Our data-model comparison suggests that there was a time lag of several decades (typically  
 476 50 years) between the climate signal and the environmental response. If this time lag is highly  
 477 probable, its duration and origin require further investigation. It may indeed result from the  
 478 resilience of plants to climate change but we cannot exclude the memory effect of aquifers  
 479 already observed by Aguiar et al. (2010) that may induce a delay between the climate signal  
 480 and its effects on ecosystems. The uncertainty associated with the ages, whether it comes  
 481 from the data or from the modelling, can also play a role by increasing or reducing this  
 482 response time.

483

#### 484 **4.2.2 The Savannah zone:**

485

486 As the ITCZ moved to more southerly latitudes, some of the drought events reconstructed in  
 487 the Sahel had a major impact in the Savannah zone. Here, data is particularly sparse and, as in  
 488 the Sahel, changes in vegetation are hardly distinguishable in these already highly degraded  
 489 environments, such as at Lake Sélé (Salzmann et al. 2005). It is at Lake Petpenoun (Catrain  
 490 2021) that the evidence is the clearest due to the presence of a gallery forest and pronounced  
 491 hydrological changes at the core site.

492 We find that the last step of degradation of the savannah vegetation occurred during event 3  
 493 also observed in the Sahel. Events 2 (1447-1493CE), 4 (1643-1657CE) and 5 (1691-1707CE)  
 494 correspond only to phases of hydrological degradation that are not reflected in the regional  
 495 vegetation. Data are still too rare to generalize this observation to the entire Savannah zone  
 496 and could only account for local conditions.

497

#### 498 **5. Conclusion**

499

500 Despite the uncertainties associated with data scarcity and heterogeneity, our study shows a  
 501 remarkable agreement between the data and our past1000 model experiments for  
 502 reconstructing the climate and environmental changes in response to natural forcing that  
 503 characterized the LIA in western Africa. It highlights a North-South contrast between the  
 504 dryness of the Sahel and the humidity of the equatorial zone. Despite the major difficulty  
 505 related to the type of vegetation at play in the Sahel and the Savannah zone already degraded  
 506 since the end of the AHP, major steps in the degradation of the environment can be identified.  
 507 Our most remarkable results consists in (1) the identification of two early warning signals at

508 1170 and 1240CE, i.e. prior to the progressive LIA drying of the Sahel that lead to the climatic  
 509 tipping point at 1800-1850CE. This tipping point marks the setting of arid conditions (the driest  
 510 condition since 850CE) which still persist today; (2) the identification of abrupt drought events  
 511 which punctuated the LIA, the most important of them has impacted both the Sahel and the  
 512 Savannah zone ca. 1600CE. The consistency between proxy records and our model  
 513 experiments suggests a strong role of large volcanic eruptions in shaping Sahel environmental  
 514 changes over the pre-industrial millennium. Further work relying on large ensembles of  
 515 climate and vegetation models will help assess such hypothesis.

516

#### 517 **Code availability**

518

519 The IPSL-CM6A-LR model code used in this work was frozen (version 6.1.0) and subsequently  
 520 altered only for correcting diagnostics or allowing further options and configurations. Versions  
 521 6.1.0 to 6.1.11 are therefore bit-reproducible for a given domain decomposition, compiling  
 522 options and supercomputer. LMDZ, XIOS, NEMO and ORCHIDEE are released under the terms  
 523 of the CeCILL licence. OASIS-MCT is released under the terms of the Lesser GNU General Public  
 524 License (LGPL). IPSL-CM6A-LR code (version 6.1.0) is publicly available through Apache  
 525 Subversion (svn) control system, with the following command lines under Linux: `svn co`  
 526 `http://forge.ipsl.jussieu.fr/igcmg/svn/modipsl/trunk modipsl; cd modipsl/util; ./model`  
 527 `IPSLCM6.1.11-LR` (IPSL-CM model development team, 2021). The `mod.def` file provides  
 528 information regarding the different revisions used, namely (1) NEMOGCM branch  
 529 `nemov36STABLE` revision 9455; (2) XIOS2 branches/`xios-2.5` revision 1873; (3) IOIPSL/src svn  
 530 tags/`v224`; (4) LMDZ6 branches/`IPSLCM6.0.15` rev 3643; (5) tags/`ORCHIDEE20/ORCHIDEE`  
 531 revision 6592; (6) OASIS3-MCT 2.0branch (rev 4775 IPSL server). The login and password  
 532 combination requested at first use to download the ORCHIDEE component is “anonymous”  
 533 and “anonymous”. We recommend referring to the project website,  
 534 [http://forge.ipsl.jussieu.fr/igcmg\\_doc/wiki/Doc/Config/IPSLCM6](http://forge.ipsl.jussieu.fr/igcmg_doc/wiki/Doc/Config/IPSLCM6) (IGCMG, 2022), for a proper  
 535 installation and compilation of the environment (version 6.1.10).

536

#### 537 **Data availability**

538

539 Pollen data are available on the African Pollen Database website:  
 540 <https://africanpollendatabase.ipsl.fr>. The other paleo-data are from the literature.

541

542 The IPSL-CM6A-LR model data and pre-processed model and proxies datasets used in this  
 543 study are available at: <https://doi.org/10.5281/zenodo.7003853>

544

#### 545 **Author contribution**

546

547 AML and MK designed the study. MK performed the IPSL-CM6A-LR model past1000  
 548 simulations and JV the simulations analysis. MC and AML collected and analyzed the data.  
 549 AML prepared the manuscript with contributions from all co-authors.

550

#### 551 **Competing interests**

552

553 The authors declare that they have no conflict of interest

554

## 555 Acknowledgements

556

557 This work contributes to the ACCEDE ANR Belmont Forum project (18 BELM 0001 05). This  
 558 work was undertaken in the framework of the French L-IPSL LABEX and the IPSL Climate  
 559 Graduate School EUR and benefited from the FNS "SYNERGIA EffeCts of lArge voLcanic  
 560 eruptions on climate and societies: UnDerstanding impacts of past Events and related  
 561 subsidence cRises to evaluate potential risks in the future" (CALDERA) project under French  
 562 CNRS grant agreement number CRSII5\_183571 – CALDERA. MK acknowledges support from  
 563 the HPC resources of TGCC under the allocations 2020-A0080107732 and 2021-A0100107732  
 564 (project gencmip6) provided by GENCI (Grand Equipement National de Calcul Intensif) and  
 565 2020225424 provided by PRACE (Partnership for Advanced Computing in Europe). This study  
 566 benefited from the ESPRI computing and data centre (<https://mesocentre.ipsl.fr>) which is  
 567 supported by CNRS, Sorbonne Université, Ecole Polytechnique and CNES as well as through  
 568 national and international grants. Thanks are due to the African Pollen Database for data  
 569 access. AML, MC and JV were funded by CNRS, and MK by IRD. We acknowledge the World  
 570 Climate Research Programme's Working Group on Coupled Modelling.

571

## 572 References

- 573 Aguiar, L., Garneau, M., Lézine, A.-M., Maugis, P.: Evolution de la nappe des sables  
 574 quaternaires dans la région des Niayes du Sénégal (1958-1994) : relation avec le climat  
 575 et les impacts anthropiques. *Sécheresse* 21, 1-8, 10.1684/sec.2010.0237, 2010.
- 576 Aumont, O., Éthé, C., Tagliabue, A., Bopp, L., and Gehlen, M.: PISCES-v2. An ocean  
 577 biogeochemical model for carbon and ecosystem studies. *Geosci. Model Develop.*, 8(8),  
 578 2465-2513, 10.5194/gmd-8-2465-2015, 2015.
- 579 Ballouche, A.: Dynamique des paysages végétaux sahélo-soudaniens et pratiques agro-  
 580 pastorales à l'Holocène : exemples au Burkina Faso. *Bull. Asso. Géogr. Français*, 75(2),  
 581 191-200, 1998.
- 582 Bertaux, J., Sifeddine, A., Schwartz, D., Vincens, A., and Elenga, H.: Enregistrement  
 583 sédimentologique de la phase sèche d'Afrique Equatoriale c. 3000 BP par la  
 584 spectrométrie IR dans les lacs Sinnda et Kitina (Sud Congo). In « Dynamique à long terme  
 585 des écosystèmes forestiers intertropicaux », Paris, ORSTOM, pp. 213-215, 1998.
- 586 Boucher, O., Servonnat, J., Albright, A.L., Aumont, O., Balkanski, Y., Bastrikov, V., Bekki, S.,  
 587 Bonnet, R., Bony, S., Bopp, L. et al.: Presentation and evaluation of the IPSL-CM6A-LR  
 588 climate model. *J. Adv. Model Earth Syst.*, 12(7), e2019MS002010,  
 589 10.1029/2019MS002010, 2020.
- 590 Brncic, T.M., Willis, K.J., Harris, D.J., and Washington, R.: Culture or climate? The relative  
 591 influences of past processes on the composition of the lowland Congo rainforest.  
 592 *Philosoph. Trans. Royal Soc. B., Biol. Sci.*, 362(1478), 229-242, 10.1098/rstb.2006.1982,  
 593 2007.
- 594 Brncic, T.M., Willis, K.J., Harris, D.J., Telfer, M.W., and Bailey, R. M.: Fire and climate change  
 595 impacts on lowland forest composition in northern Congo during the last 2580 years  
 596 from palaeoecological analyses of a seasonally flooded swamp. *Holocene*, 19, 79–89,  
 597 10.1177/0959683608098954, 2009.
- 598 Carré, M., Azzoug, M., Zaharias, P., Camara, A., Cheddadi, R., Chevalier, M., Fiorillo, D., Gaye,  
 599 A.T., Janicot, S., Khodri, M., Lazar, A., Lazareth, C.E., Mignot, J., Mitma Garcia, N., Patris,  
 600 N., Perrot, O., and Wade, M.: Modern drought conditions in western Sahel

- 601           unprecedented in the past 1600 years. *Climate Dynamics*, 52(3), 1949-1964,  
602           10.1007/s00382-018-4311-3, 2019.
- 603   Catrain, M.: *Le Petit Age de Glace en Afrique équatoriale : apport de l'étude palynologique des*  
604           *sédiments du lac de Petpenoun, Cameroun. Unpublished Ms Thesis. University of Paris*  
605           *Saclay, 2021.*
- 606   Coquery-Vidrovitch, C.: *Écologie et histoire en Afrique noire. Histoire, économie et société,*  
607           483-504, 1997.
- 608   Descroix, L., Diogue Niang, A., Panthou, G., Bosdian, A., Sane, Y., Dacosta, H., Malam Abdou,  
609           M., Vandervaere, J.P., and Quantin, G.: *Evolution récente de la pluviométrie en Afrique*  
610           *de l'Ouest à travers deux regions: la Sénégalie et le bassin du Niger moyen.*  
611           *Climatologie* 12, 25-43, 2015.
- 612   d'Orgeval, T., Polcher, J., and de Rosnay, P.: *Sensitivity of the West African hydrological cycle*  
613           *in ORCHIDEE to infiltration processes. Hydro. Earth Syst. Sci.,* 12(6), 1387-1401,  
614           10.5194/hess-12-1387-2008, 2008.
- 615   Demenocal, P., Ortiz, J., Guilderson, T., Adkins, J., Sarnthein, M., Baker, L., and Yarusinsky, M.:  
616           *Abrupt onset and termination of the African Humid Period: rapid climate responses to*  
617           *gradual insolation forcing. Quatern. Sci. Rev.,* 19(1-5), 347-361, 10.1016/S0277-  
618           3791(99)00081-5, 2000.
- 619   Deser C., Alexander, M.A., Xie, S.P., et al.: *Sea surface temperature variability: Patterns and*  
620           *mechanisms. Annual review of Marine Science* 2, 115–143. 10.1146/annurev-marine-  
621           120408-151453, 2010.
- 622   Elenga, H.: *Végétation et climat du Congo depuis 24 000 ans B. P: analyse palynologique de*  
623           *séquences sédimentaires du Pays Bateke et du littoral. PhD, Aix-Marseille III, 1992.*
- 624   Elenga, H., Schwartz, D., Vincens, A., Bertaux, J., de Namur, C., Martin, L., Wirrmann, D., and  
625           Servant, M.: *Diagramme pollinique holocène du lac Kitina (Congo): mise en évidence de*  
626           *changements paléobotaniques et paléoclimatiques dans le massif forestier du*  
627           *Mayombe. C. R. Acad. Sci., Série 2a,* 323, 403-410, 1996.
- 628   Fofana, C.A.K., Sow, E., and Lézine, A.-M.: *The Senegal River during the last millennium. Rev.*  
629           *Palaeobot. Palynol.* 275, 104175, 10.1016/j.revpalbo.2020.104175, 2020.
- 630   Folland, C.K., Palmer, T.N., and Parker, D.E.: *Sahel rainfall and worldwide sea temperatures,*  
631           1901–85. *Nature*, 320, 602–607, 10.1038/320602a0, 1986.
- 632   Gadgil, S.: *The monsoon system: Land–sea breeze or the ITCZ? J. Earth Syst. Sci.* 127, 1.  
633           10.1007/s12040-017-0916-x, 2018.
- 634   Gallego, D., Ordóñez, P., Ribera, P., Peña-Ortiz, C., and García-Herrera, R.: *An instrumental*  
635           *index of the West African Monsoon back to the nineteenth century. Quarter. J. Royal*  
636           *Meteo. Soc.,* 141(693), 3166-3176, 10.1002/qj.2601, 2015.
- 637   Giannini, A., Saravanan, R., and Chang, P.: *Oceanic forcing of Sahel rainfall on interannual to*  
638           *interdecadal time scales. Science,* 302, 1027–1030, 10.1126/science.1089357, 2003.
- 639   Holmes, J.A., Allen, M.J., Street-Perrott, F.A., Ivanovich, M., Perrott, R.A., and Waller, M.P.:  
640           *Late Holocene palaeolimnology of Bal Lake, northern Nigeria, a multidisciplinary study.*  
641           *Palaeogeogr., Palaeoclimatol., Palaeoecol.,* 148(1-3), 169-185, 10.1016/S0031-  
642           0182(98)00182-5, 1999.
- 643   Hourdin, F., Rio, C., Grandpeix, J.Y., Madeleine, J.B., Cheruy, F., Rochetin, N., Jam, A., Musat,  
644           I., Idelkadi, A., Fairhead, L., Foujols, M.A., Mellul, L., Traore, A.K., Dufresne, J.L., Boucher,  
645           O., Lefebvre, M.P., Millour, E., Vignon, E., Jouhaud, J., Diallo, F.B., Lott, F., Gastineau, G.,  
646           Caubel, A., Meurdesoif, Y., and Ghattas, J.: *LMDZ6A: the atmospheric component of the*

- 647 IPSL climate model with improved and better tuned physics. *J. Adv. Model. Earth Syst.*  
 648 12(7): e2019MS001892, 10.1029/2019MS001892, 2020.
- 649 Jungclauss, J. H., Bard, E., Baroni, M., Braconnot, P., Cao, J., Chini, L. P., Egorova, T., Evans, M.,  
 650 Gonzalez-Rouco, J.F., Goose, H., Hurtt, G.C., Joos, F., Kaplan, J.O., Khodri, M., Goldewijk,  
 651 K.K., Krivova, N., LeGrance, A.N., Lorenz, S.J., Luterbacher, J., Man, W., Maucock, A.C.,  
 652 Mainshausen, M., Moberg, A., Muscheler, R., Nehbass-Ahles, C., Otto-Bliesner, B.I.,  
 653 Phipps, S.J., Pongratz, J., Rozanov, E., Schmidt, G.A., Schmidet, H., Schmutz, W., Schurer,  
 654 A., Shapiro, A.I., Sigl, M., Smerdon, J.E., Solanki, S.K., Timmreck, C., Toohey, M., Usoskin,  
 655 ILGL, Wagner, S., Wu, C.J., Yeo, K.L., Zanchettin, D., Zhang, Q., and Zorita, E. : The PMIP4  
 656 contribution to CMIP6–Part 3: The last millennium, scientific objective, and  
 657 experimental design for the PMIP4 past1000 simulations. *Geosci. Model Dev.*, 10(11),  
 658 4005-4033. 10.5194/gmd-10-4005-017, 2017.
- 659 Kageyama, M., Albani, S., Braconnot, P., Harrison, S. P., Hopcroft, P. O., Ivanovic, R. F.,  
 660 Lambert, F., Marti, O., Peltier, W.R., Peterschmitt, J.Y., Roche, D.M., Tarasov, L., Zhang,  
 661 X., Brady, E.C., Haywood, A.M., LeGrande, A.N., Lunt, D.J., Mahowald, N.M.,  
 662 Mikolajewicz, U., Nisancioglu, K.H., Otto-Bliesner, B.L., Renssen, H., Tomas, R.A., Zhang,  
 663 Q., Abe-Ouchi, A., Bartlein, P.J., Cao, J., Li, Q., Lohmann, G., Ohgaito, R., Shi, X., Volodin,  
 664 E., Yoshida, K., Zhang, X., and Zheng, W. : The PMIP4 contribution to CMIP6–Part 4:  
 665 Scientific objectives and experimental design of the PMIP4-CMIP6 Last Glacial Maximum  
 666 experiments and PMIP4 sensitivity experiments. *Geosci. Model Dev.*, 10(11), 4035-4055,  
 667 10.5194/gmd-10-4035-2017, 2017.
- 668 Kanamitsu, M., Ebisuzaki, W., Woollen, J., Yang, S.-K., Hnilo, J.J., Fiorino, M., and Potter, G.L.:  
 669 NCEP-DOE AMIP-II Reanalysis (R-2), *Bull. Amer. Meteor. Soc.*, 83, 1631-1643,  
 670 0.1175/BAMS-83-11-1631, 2002
- 671 Kucharski, F., Molteni, F., King, M.P., Farneti, R., Kang, I.S., and Feudale, L.: On the need of  
 672 intermediate complexity general circulation models : A “SPEEDY” example. *Bull. Amer.*  
 673 *Meteo. Soc.*, 94(1), 25-30, 10.1175/BAMS-D-11-00238.1, 2013.
- 674 Lawrence, D. M., Hurtt, G. C., Arneeth, A., Brovkin, V., Calvin, K. V., Jones, A. D., Jones, C. D.,  
 675 Lawrence, P. J., de Noblet-Ducoudré, N., Pongratz, J., Seneviratne, S. I., and Shevliakova,  
 676 E.: The Land Use Model Intercomparison Project (LUMIP) contribution to CMIP6:  
 677 rationale and experimental design, *Geosci. Model Dev.*, 9, 2973–2998,  
 678 <https://doi.org/10.5194/gmd-9-2973-2016>, 2016.
- 679 Le Borgne, J.: Un exemple d'invasion polaire sur la région mauritano-sénégalaise. *Annales*  
 680 *Géogr.*, 489, 521-548, 1979.
- 681 Lebamba, J., Vincens, A., Lézine, A.-M., Marchant, R., and Buchet, G.: Forest-savannah  
 682 dynamics on the Adamawa plateau (Central Cameroon) during the “African humid  
 683 period” termination : A new high-resolution pollen record from Lake Tizong. *Rev.*  
 684 *Palaeobot. Palynol.*, 235, 129-139, 10.1016/j.revpalbo.2016.10.001, 2016.
- 685 Lenton, T.M.: Early warning of climate tipping points. *Nature Climate Change* 1, 201-209,  
 686 10.1038/nclimate1143, 2011.
- 687 Lézine, A.M., Lemonnier, K., and Fofana, C.A.K.: Sahel environmental variability during the last  
 688 millennium: insight from a pollen, charcoal and algae record from the Niayes area,  
 689 Senegal. *Rev. Palaeobot. Palynol.* 271, 104103, 10.1016/j.revpalbo.2019.104103, 2019.
- 690 Lézine, A.M.: Late Quaternary vegetation and climate of the Sahel. *Quatern. Res.*, 32, 317-334,  
 691 10.1016/0033-5894(89)90098-7, 1989.
- 692 Lézine, A.M., Holl A., Lebamba J., Vincens A., Assi-Khadjis C., Février L., and Sultan  
 693 E.: Temporal relationship between Holocene human occupation and vegetation change

- 694 along the northwestern margin of the Central African rainforest. *C. R. Géosci.*, 345, 327-  
695 335, 10.1016/j.crte.2013.03.001, 2013.
- 696 Lézine, A.M., Lemonnier, K., Waller, M.P., Bouimetarhan, I., Dupont, L. and APD contributors :  
697 Changes in the West African Landscape at the end of the African Humid Period.  
698 *Palaeoecology of Africa* 35, 65-83, 10.1201/9781003162766-6, 2021
- 699 Lézine, A.M., Zheng, W., Braconnot, P., Krinner, G.: Late Holocene plant and climate evolution  
700 at Lake Yoa, northern Chad: pollen data and climate simulations. *Clim. Past* 7, 1351-  
701 1362, 10.5194/cp-7-1351-2011, 2011.
- 702 Maley, J., and Vernet, R. : *Peuples et évolution climatique en Afrique nord-tropicale, de la fin*  
703 *du Néolithique à l'aube de l'époque moderne. Afriques. Débats, Méthodes et Terrains*  
704 *d'Histoire*, 04, 10.4000/afriques.1209, 2013.
- 705 Matthes, K., Funke, B., Andersson, M. E., Barnard, L., Beer, J., Charbonneau, P., Clilverd, M. A.,  
706 Dudok de Wit, T., Haberreiter, M., Hendry, A., Jackman, C. H., Kretzschmar, M.,  
707 Kruschke, T., Kunze, M., Langematz, U., Marsh, D. R., Maycock, A. C., Misios, S., Rodger,  
708 C. J., Scaife, A. A., Seppälä, A., Shanguan, M., Sinnhuber, M., Tourpali, K., Usoskin, I.,  
709 van de Kamp, M., Verronen, P. T., and Versick, S.: Solar forcing for CMIP6 (v3.2), *Geosci.*  
710 *Model Dev.*, 10, 2247–2302, <https://doi.org/10.5194/gmd-10-2247-2017>, 2017.
- 711 McPhaden, M.J., Zebiak, S.E., and Glanz, M.H.: ENSO as an integrating concept in earth  
712 science. *Science*, 314, 5806, 1740-1745, 10.1126/science.1132588, 2006.
- 713 Meinshausen, M., Vogel, E., Nauels, A., Lorbacher, K., Meinshausen, N., Etheridge, D. M.,  
714 Fraser, P. J., Montzka, S. A., Rayner, P. J., Trudinger, C. M., Krummel, P. B., Beyerle, U.,  
715 Canadell, J. G., Daniel, J. S., Enting, I. G., Law, R. M., Lunder, C. R., O'Doherty, S., Prinn,  
716 R. G., Reimann, S., Rubino, M., Velders, G. J. M., Vollmer, M. K., Wang, R. H. J., and Weiss,  
717 R.: Historical greenhouse gas concentrations for climate modelling (CMIP6), *Geosci.*  
718 *Model Dev.*, 10, 2057–2116, <https://doi.org/10.5194/gmd-10-2057-2017>, 2017.
- 719 Mohino, E., Janicot, S., and Bader, J.: Sahel rainfall and decadal to multi-decadal sea surface  
720 temperature variability. *Clim. Dyn.*, 37(3), 419-440, 10.1007/s00382-010-0867-2, 2011.
- 721 Mulitza, S., Heslop, D., Pittauerova, D., Fischer, H. W., Meyer, I., Stuut, J. B., Zabel, M.,  
722 Mollenhauer, G., Collins, J.A., Kuhnert, H., and Schulz, M.: Increase in African dust flux  
723 at the onset of commercial agriculture in the Sahel region. *Nature*, 466(7303), 226-228,  
724 10.1038/nature09213, 2010.
- 725 Nash, D.J., De Cort, G., Chase, B.M., Verschuren, D., Nicholson, S.E., Shanahan, T.M., Asrat,  
726 A., Lézine, A.M., and Grab, S.W.: African hydroclimatic variability during the last 2000  
727 years. *Quatern. Sci. Rev.*, 154, 1-22, 10.1016/j.quascirev.2016.10.012, 2016.
- 728 Ngomanda, A., Jolly, D., Bentaleb, I., Chepstow-Lusty, A., M'voubou Makaya, Maley, J.,  
729 Fontune, M., Oslisly, R., Rabenkogo, N.: Lowland forest response to hydrological changes  
730 during the last 1500 years in Gabon, Western Equatorial Africa. *Quatern. Res.* 60, 411-  
731 425, 10.1016/j.yqres.2008.12.002, 2007.
- 732 Nguetsop, V. F., Bentaleb, I., Favier, C., Martin, C., Bietrix, S., Giresse, P., Servant-Vildary, M.,  
733 and Servant, M.: Past environmental and climatic changes during the last 7200 cal yr BP  
734 in Adamawa plateau (Northern-Cameroun) based on fossil diatoms and sedimentary  
735 carbon isotopic records from Lake Mbalang. *Clim. Past*, 7(4), 1371-1393, 10.5194/cp-7-  
736 1371-2011, 2011.
- 737 Nguetsop, V.F., Bentaleb, I., Favier, C., Bietrix, S., Martin, C., Servant-Vildary, S., and Servant,  
738 M.: A late Holocene palaeoenvironmental record from Lake Tizong, northern Cameroon  
739 using diatom and carbon stable isotope analyses. *Quatern. Sci. Rev.*, 72, 49-62,  
740 10.1016/j.quascirev.2013.04.005, 2013.



- 741 Nguetsop, V.F., Servant-Vildary, S., Servant, M., and Roux, M.: Long and short-time scale  
742 climatic variability in the last 5500 years in Africa according to modern and fossil diatoms  
743 from Lake Ossa (Western Cameroon). *Global Planet. Change*, 72(4), 356-367,  
744 10.1016/j.gloplacha.2010.01.011, 2010.
- 745 Nicholson, S.E.: The West African Sahel: A review of recent studies on the rainfall regime and  
746 its interannual variability. *Intern. Scholar. Res. Not.*, 453521, 10.1155/2013/453521,  
747 2013.
- 748 Nicholson, S.E.: Climatic variations in the Sahel and other African regions during the past five  
749 centuries. *J. Arid Env.*, 1(1), 3-24, 10.1016/S0140-1963(18)31750-6, 1978.
- 750 Nicholson, S.E.: The nature of rainfall fluctuations in subtropical West Africa. *Monthly Weather*  
751 *Rev.*, 108(4), 473-487, 10.1175/1520-0493(1980)108<0473:TNORFI>2.0.CO;2, 1980.
- 752 Nicholson, S.E.: The West African Sahel: A review of recent studies on the rainfall regime and  
753 its interannual variability. *Intern. Scholar. Res. Notices*, 2013, 453521,  
754 10.1155/2013/453521, 2013.
- 755 Nicholson, S.E., Klotter, D., and Dezfuli, A.K.: Spatial reconstruction of semi-quantitative  
756 precipitation fields over Africa during the nineteenth century from documentary  
757 evidence and gauge data. *Quat. Res.*, 78, 13–23, 10.1016/j.yqres.2012.03.012, 2012
- 758 Pham-Duc, B., Sylvestre, F., Papa, F., Frappart, F., Bouchez, C. and Crétaux, J.F.: The Lake Chad  
759 hydrology under current climate change. *Nature scientific Reports* 10, 5498, /s41598-  
760 020-62417-w, 2020.
- 761 Reynaud-Farrera, I., Maley, J., and Wirrmann, D.: Végétation et climat dans les forêts du Sud-  
762 Ouest Cameroun depuis 4770 ans BP : analyse pollinique des sédiments du Lac Ossa. *CR*  
763 *Acad. Sci. Paris*, 322(série II a), 749-755, 1996.
- 764 Rodríguez-Fonseca, B., Mohino, E., Mechoso, C. R., Caminade, C., Biasutti, M., Gaetani, M.,  
765 Garcia-Serrano J., Vízny E. K., Cook K., Xue Y. K., Polo I., Losada T., Druyan L., Fontaine B.,  
766 Bader J., Doblas-Reyes F. J., Goddard L., Janicot Serge, Arribas A., Lau W., Colman A.,  
767 Vellinga M., Rowell D. P., Kucharski F., and Voltaire, A. : Variability and predictability of  
768 West African droughts: a review on the role of sea surface temperature anomalies. *J.*  
769 *Clim.*, 28(10), 4034-4060, 10.1175/JCLI-D-14-00130.1., 2015.
- 770 Rousset, C., Vancoppenolle, M., Madec, G., Fichefet, T., Flavoni, S., Barthélemy, A., Benshila,  
771 R., Chanut, J., Lévy, C., Masson, S., and Vivier, F.: The louvain-la-neuve sea ice model  
772 LIM3.6: global and regional capabilities. *Geosci. Model. Dev.* 8(10), 2991–3005,  
773 10.5194/gmd-8-2991-2015, 2015.
- 774 Salzmann, U., and Hoelzmann, P.: The Dahomey Gap: an abrupt climatically induced rain forest  
775 fragmentation in West Africa during the late Holocene. *Holocene*, 15(2), 190-199,  
776 10.1191/0959683605hl799rp, 2005.
- 777 Schefuß, E., Schouten, S., and Schneider, R.R.: Climatic controls on central African hydrology  
778 during the past 20,000 years. *Nature*, 437(7061), 1003-1006, 10.1038/nature03945,  
779 2005.
- 780 Shanahan, T.M., Overpeck, J.T., Anchukaitis, K.J., Beck, J.W., Cole, J.E., Dettman, D.L., Peck,  
781 J.A., Scholz, A., and King, J.W.: Atlantic forcing of persistent drought in West Africa.  
782 *Science*, 324(5925), 377-380, 10.1126/science.1166352, 2009.
- 783 Street-Perrott, F.A., Holmes, J.A., Waller, M.P., Allen, M.J., Barber, N.G.H., Fothergill, P. A.,  
784 Harkness, D.D., Ivanovich, M., Kroon, D. and Perrott, R.A.: Drought and dust deposition  
785 in the West African Sahel: a 5500-year record from Kajemarum Oasis, northeastern  
786 Nigeria. *Holocene*, 10(3), 293-302, 10.1191/095968300678141274, 2000.

- 787 Tovar, C., Harris, D.J., Breman, E., Brncic, T., and Willis, K.J.: Tropical monodominant forest  
788 resilience to climate change in Central Africa: A *Gilbertiodendron dewevrei* forest pollen  
789 record over the past 2,700 years. *J. Veget. Sci.*, 30(3), 575-586, 10.1111/jvs.12746, 2019.
- 790 Toohey, M., and Sigl, M.: Volcanic stratospheric sulfur injections and aerosol optical depth  
791 from 500 BCE to 1900 CE, *Earth Syst. Sci. Data*, 9, 809–831, 10.5194/essd-9-809-2017,  
792 2017.
- 793 Villamayor, J., Mohino, E., Khodri, M., Mignot, J., and Janicot, S.: Atlantic control of the late  
794 nineteenth-century Sahel humid period. *J. Clim.*, 31(20), 8225-8240, 10.1175/JCLI-D-18-  
795 0148.1, 2018.
- 796 Vincens, A., Buchet, G., Elenga, H., Fournier, M., Martin, L., de Namur, C., Schwartz, D., Servant,  
797 M., and Wirrmann, D.: Changement majeur de la végétation du lac Sinnda (vallée du  
798 Niari, Sud Congo) consécutif à l'assèchement climatique holocène supérieur : apport de  
799 la palynologie. *C.R. Acad. Sci. Paris*, 318, 1521-1526, 1994.
- 800 Vincens, A., Schwartz, D., Bertaux, J., Elenga, H., and de Namur, C.: Late Holocene climatic  
801 changes in western equatorial Africa inferred from pollen from Lake Sinnda, southern  
802 Congo. *Quatern. Res.* 50(1), 34-45, 10.1006/qres.1998.1979, 1998.
- 803 Vincens, A., Schwartz, D., Elenga, H., Reynaud-Farrera, I., Alexandre, A., Bertaux, J., Mariotti,  
804 A., Martin, L., Meunier, J.D., Nguetsop, F., Servant, M., Servant-Vildary, S., and  
805 Wirrmann, D.: Forest response to climate changes in Atlantic Equatorial Africa during  
806 the last 4000 years BP and inheritance on the modern landscapes. *J. Biogeogr.*, 26(4),  
807 879-885, 10.1046/j.1365-2699.1999.00333.x, 1999.
- 808 Waller, M.P., Street-Perrott, F.A., and Wang, H.: Holocene vegetation history of the Sahel:  
809 pollen, sedimentological and geochemical data from Jikariya Lake, north-eastern  
810 Nigeria. *J. Biogeogr.*, 34(9), 1575-1590, 0.1111/j.1365-2699.2007.01721.x, 2007.
- 811 Wang, H., Holmes, J.A., Street-Perrott, F.A., Waller, M.P., and Perrott, R. A. Holocene  
812 environmental change in the West African Sahel: sedimentological and mineral-  
813 magnetic analyses of lake sediments from Jikariya Lake, northeastern Nigeria. *J.*  
814 *Quatern. Sci.*, 23(5), 449-460, 10.1002/jqs.1154, 2008.
- 815
- 816